Arabian Journal of Geosciences (2024) 17:6
https://doi.org/10.1007/s12517-023-11784-5

ORIGINAL PAPER

Groundwater investigation within the basement complex, North Central Nigeria, using magnetic and resistivity method

Adebayo Abbass Adetona[1] · Shakira B. Aliyu[1] · Fidelis I. Kwaghhua[1] · Luka M. Damidami[2]

Received: 14 September 2022 / Accepted: 9 November 2023

Abstract

The research focuses on using an integrated approach to locate viable locations for sitting boreholes within the Bosso local government area of Niger State. An area within the basement complex in North Central Nigeria is enclosed by longitudes 6.25′ to 6.31′ and latitudes 9.35′ to 9.45′, with a total area of 16 by 8 km^2. This work is central to employing both magnetic and electrical methods of exploration. The derivatives of residual magnetic intensity data for the area were employed to locate regions within the area that are fractured or faulted and could give access to the required underground water. This was followed by conducting Vertical Electrical Sounding (Schlumberger array) within two selected sites within the faulted area and one site outside the faulted area to serve as a control. First vertical derivative displayed lineaments labelled (A), (B), (C), (D), (F), and (G), which are mostly in the Northeast–Southwest (NE-SW) direction. Three sites were chosen for Vertical Electrical investigation for groundwater; sites A (on latitudes 9° 40′ 37.11″ to 9° 41′ 37.1″ N and longitudes 6° 29′ 52.64″ to 6° 30′ 51.56″ E) and B (latitudes 09° 40′ 37.17″ to 09° 41′ 37.15″ N and longitudes 06° 29′ 51.66″ to 06° 30′ 51.55″ E) are within the fractured zones and site C is outside the fractured zone which serves as a control. Thirty-six (36) VES points were sampled on each of the three sites measuring 500 by 500 m^2. Result of Vertical Electrical Sounding carried out indicated three geologic layers comprised of topsoil, intermediate clay formation, and weathered/fractured or fresh basement. The depth of the basement at VES points within sites A and B varies from 25 to 48 m; these are within the faulted zone, while depth of overburden in site C used for control varies from 6 to 18 m. Hence, VES points located within sites A (1) and B (2) are viable for groundwater exploration; points A_2, A_5, B_4, B_5, C_2, C_4, D_4, D_5, E_1, E_3, and F_4 are high conductivity zone which are prolific for groundwater potential. The depth range for aquifer potential zones is between 22.7 and 50.4 m. Result from site C equally shows two layers, more than 90% of the VES which are not viable for groundwater potential. This work thus recommends sitting of borehole within VES points on site A or B for good yield and authenticates the viability of integrated algorithms for groundwater exploration in the basement complex region.

Keywords Anomalous Magnetic Field (AMF) · Aquifer potential · Geoelectric section · Iso-resistivity · Vertical Electrical Sounding (VES)

Responsible Editor: Broder J. Merkel

✉ Adebayo Abbass Adetona
tonabass@gmail.com

Shakira B. Aliyu
shakirat@futminna.edu.ng

Fidelis I. Kwaghhua
fidelisik@gmail.com

Luka M. Damidami
damiresist2@gmail.com

[1] Department of Applied Geophysics, School of Physical Science, Federal University of Technology Minna, Minna, Niger State, Nigeria

[2] Centre for Extramural and Remedial Studies (CEPES), Federal University of Technology Minna, Minna, Niger State, Nigeria

Published online: 07 December 2023

Introduction

More than 300 million people within African local communities today lack access to portable fresh water (Water for Africa 2010). Aqueducts or canals are occasionally used to transport water from far-off surface water sources such as streams, rivers, lakes, or reservoirs to enable communities to meet their daily water needs (Plummer et al. 1999; Water for Africa 2010). Another important and more improved source is groundwater, the water that lies beneath the ground surface, filling the pore space between grains in bodies of sediment and clastic sedimentary rock, and filling cracks and crevices in all types of rock. The source of groundwater is rain and snow that fall to the ground. Groundwater is, therefore, a tremendous major economic resource, particularly in most cities of Nigeria where portable water is scarce. Many homes and organizations pump their required quantities of water from the ground because groundwater is commonly less polluted and more economical to use than surface water (Plummer et al. 1999).

Electrical resistivity survey is relevant to groundwater exploration (Olasehinde 1999; Nwankwo et al. 2004; Singh et al. 2006; Alile et al. 2008; Ariyo and Adeyemi 2009; Anudu et al. 2011; Oyedele et al. 2011). The resistivity of rocks is strongly influenced by the presence of groundwater, which acts as an electrolyte. The minerals that form the matrix of a rock are generally good resistors than groundwater, so the resistivity of sediment decreases with the amount of groundwater it contains. This depends on the fraction of the rock that consists of pore spaces and the fraction of this pore volume that is water-filled (Lowrie 1997).

The area for this study Fig. 1 lies within longitudes 6.25′ to 6.31′ and latitudes 9.35′ to 9.45′, and the area has a size of 16

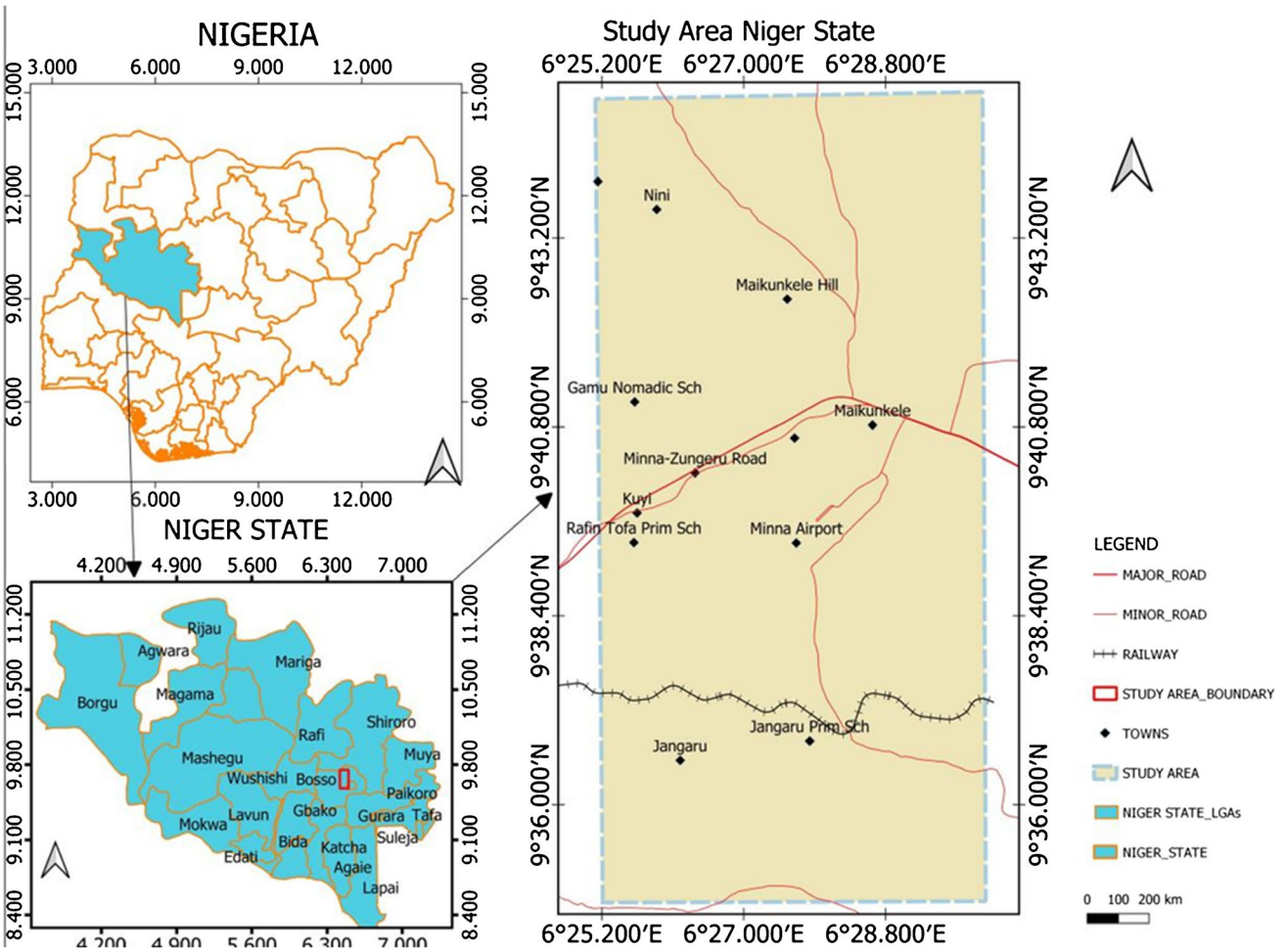

Fig. 1 Location map of the study area

by 8 km^2, located within central Nigeria basement region. The region is of interest due to the presence of some major government agencies among which are the Nigerian Airforce Base 12 and its staff residence, headquarters of Bosso local government, offices of the Independent National Electoral Commission (INEC), six public schools (primary, and tertiary), Minna International Airport. About seven communities and an estimated population of about 4000 families inhabited the area. Perennial shortage of water is a major challenge. Several boreholes sited within this region are either a complete failure or have poor yield, as a result of inadequate knowledge of the underlying aquifers (Akurugu et al. 2020; Yadav and Shashi 2007). The geology map Fig. 2. reveals the area as sitting on both outcrop and intrusive volcanic bodies of North Central Nigeria.

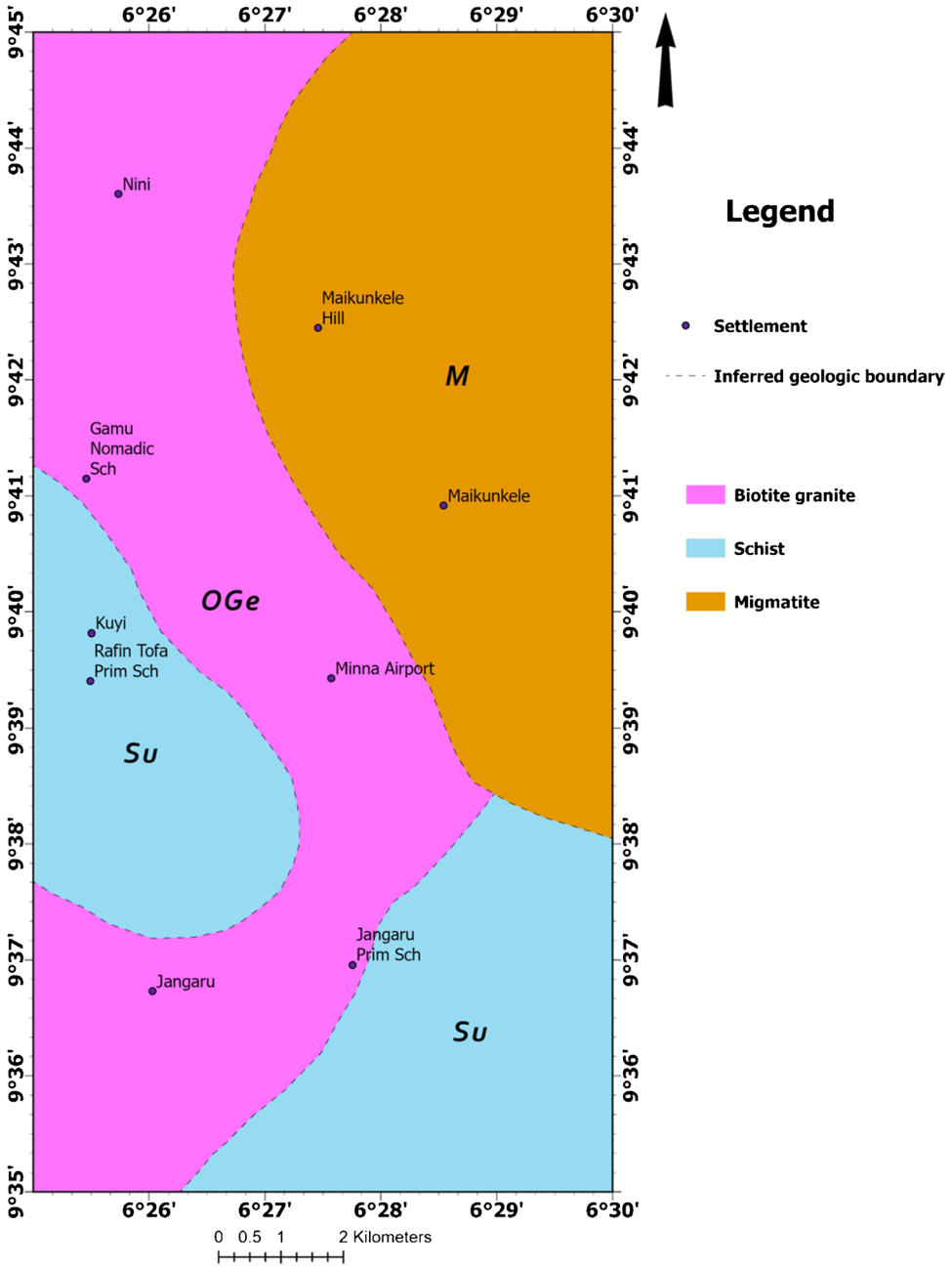

Fig. 2 Geology map of the study area

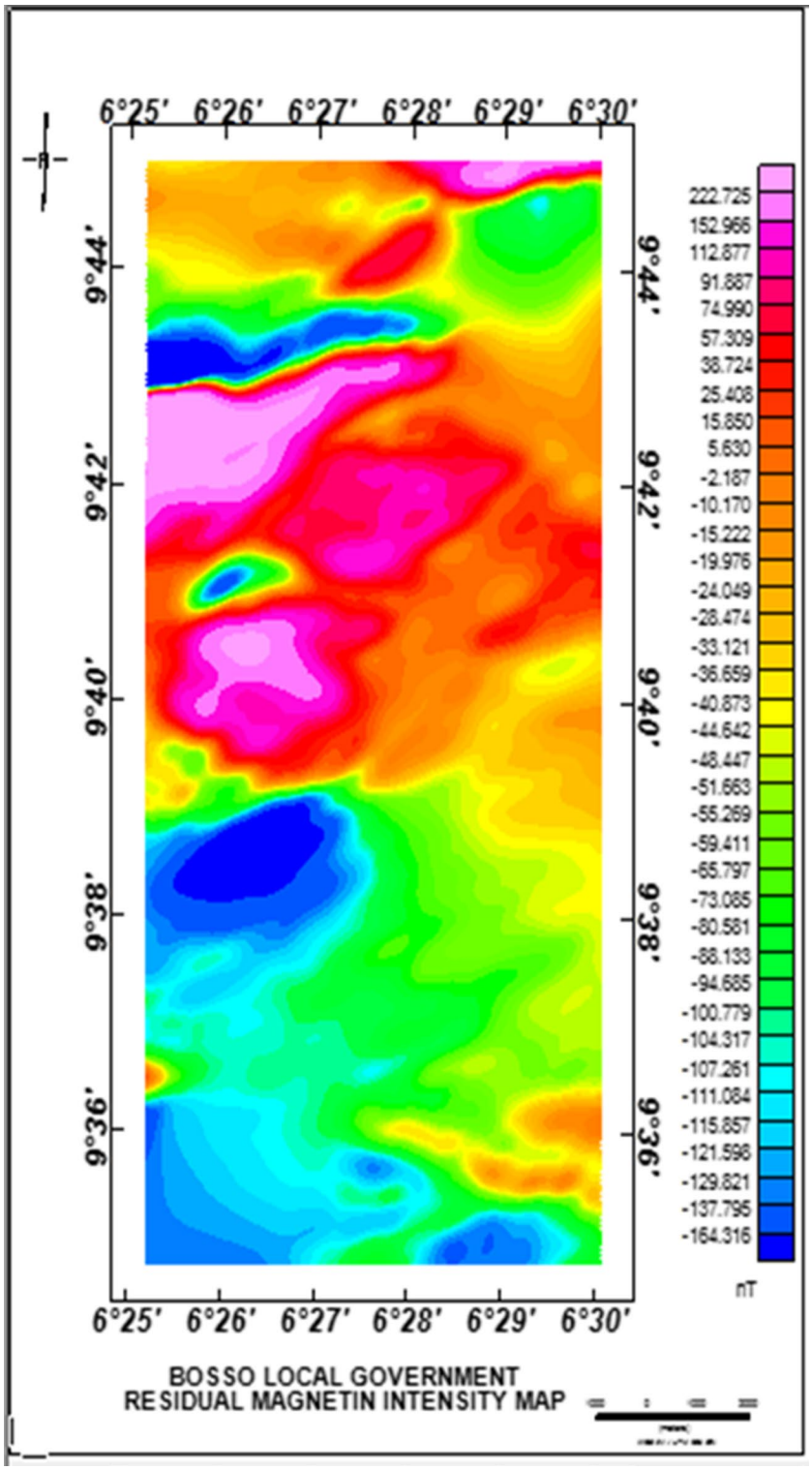

Fig. 3 Anomalous Magnetic Field (AMF) map of the study area

Table 1 Summary of VES results along profile A in the study area for Field 1

VES station	No of layer	Layer average resist(Ωm)	Thickness (m)	Depth (m)	Type of curve	Inferred lithology
A_1	1	38.3	20.0	0.5	A	Topsoil (clayey sand)
	2	1065.1	20.0	40.0		Weathered basement
	3	2915.3	∞	∞		Fresh basement
A_2	1	3.4	0.3	0.3	K	Topsoil (clayey sand)
	2	889.05	11.65	11.95		Clay
	3	5.6	∞	∞		Weathered bedrock
A_3	1	171.0	0.3	0.3	K	Topsoil
	2	253.05	5.06	5.09		Clayey soil
	3	122.9	∞	∞		Weathered bedrock
A_4	1	1.4	7.0	7.0	A	Topsoil
	2	132.55	20.65	27.65		Clay
	3	2263.6	∞	∞		Weathered basement
A_5	1	3.8	0.3	0.3	A	Sandy clay
	2	237.4	4.7	5.00		Weathered basement
	3	1094.8	∞	∞		Fractured basement
A_6	1	365.9	3.0	3.0	H	Topsoil
	2	81.0	37.5	40.50		(Clayey sand)
	3	76.9	∞	∞		Weathered basement

A geophysical approach to this challenge is to sample the aeromagnetic data, employ relevant analytical algorithms to detect structures and fault lines within regions' basements, and use an appropriate ground truthing method to affirm if these fractures are interconnected and to the desired underground water (Rangganai and Ebinga 2008). Electrical resistivity survey is relevant to groundwater exploration (Olasehinde 1999; Nwankwo et al. 2004; Singh et al. 2006; Alile et al. 2008; Ariyo and Adeyemi 2009; Anudu et al. 2011; Oyedele et al. 2011). The presence of

Table 2 Summary of VES results along profile B in the study area for Field 1

VES station	No of layer	Layer average resist (Ωm)	Thickness (m)	Depth (m)	Type of curve	Inferred lithology
B_1	1	179.70	5.00	5.00	A	Topsoil (clayed sand)
	2	457.00	15.00	20.00		Clay
	3	3893.60	∞	20.00		Weathered basement
B_2	1	45.00	5.00	5.00	A	Topsoil
	2	344.15	5.00	10.00		Sandy clay
	3	1233.6	∞	10.00		Fresh basement
B_3	1	281.30	5.00	5.00	K	Topsoil
	2	405.85	5.00	10.00		Sandy clay
	3	884.40	∞	10.00		Weathered basement
B_4	1	161.20	20.00	20.00	A	Clay
	2	2001.40	10.00	30.00		Weathered basement
B_5	3	9949.50	∞	30.00	A	Fresh basement
	1	94.80	0.80	0.80		Sandy clay
	2	247.50	2.40	3.20		Weathered basement
B_6	3	3369.00	∞	3.20	H	Fresh basement
	1	127.70	1.10	1.10		Sandy clay
	2	54.32	5.10	8.30		Clay
	3	887	∞	∞		Weathered basement

Table 3 Summary of VES results along profile A in the study area for Field 2

VES station	No of layer	Layer average resist (Ωm)	Thickness (m)	Depth (m)	Type of curve	Inferred lithology
A_0	1	13.4	0.60	0.00	A	Topsoil
	2	2396.9	20.2	0.60		Consolidated clay
	3	753.3	∞	20.8		Weathered basement
A_1	1	124.9	0.9	0.00	K	Topsoil
	2	973.6	24.4	0.9		Consolidated clay
	3	266.4	∞	25.3		Weathered basement
A_2	1	101.0	1.0	0.00	A	Topsoil
	2	470.0	33.3	1.00		Weathered basement
	3	4541.8	∞	34.1		Fresh basement
A_3	1	410.4	1.8	0.00	K	Topsoil
	2	578.2	28.0	1.8		Consolidated clay
	3	568.8	∞	29.8		Weathered basement
A_4	1	86.8	0.7	0.00	A	Topsoil
	2	468.5	23.3	0.7		Clay
	3	1090.3	∞	24.00		Weathered basement
A_5	1	15.6	0.9	0.00	A	Topsoil
	2	197.2	38.5	0.9		Clay
	3	770.2	∞	39.4		Weathered basement

groundwater, which serves as an electrolyte, has a significant impact on the resistivity of rocks. The resistivity of sediment diminishes with the quantity of groundwater it contains because the minerals that make up the matrix of a rock are often better resistors than groundwater. This is dependent on the percentage of the rock that is made up of pore spaces and the percentage of this pore volume that is filled with water (Lowrie 1997).

To avoid the consistent failure of boreholes sited within the basement regions such as this, it is important that they are sited within the fracture zones and where these fractures are interconnected so that re-charging the reservoir will be

Table 4 Summary of VES results along profile B in the study area for Field 2

VES station	No of layer	Layer average resist (Ωm)	Thickness (m)	Depth (m)	Type of curve	Inferred lithology
B_0	1	56.1	0.8	0.00	K	Topsoil
	2	589.0	10.7	0.80		Clay
	3	233.2	∞	11.5		Weathered basement
B_1	1	45.7	0.6	0.00	K	Topsoil
	2	320.9	6.6	0.6		Clay
	3	270.1	∞	7.2		Weathered basement
B_2	1	372.5	3.7	0.00	Q	Topsoil
	2	340.6	7.7	3.7		Clay
	3	171.2	∞	11.4		Weathered basement
B_3	1	40.2	0.6	0.00	A	Topsoil
	2	272.7	13.6	0.60		Clay
	3	457.7	∞	14.2		Weathered basement
B_4	1	180.6	1.0	0.00	A	Topsoil
	2	422.3	21.4	1.0		Clay
	3	3011.7	∞	22.4		Fresh Basement
B_5	1	69.2	8.7	0.00	A	Topsoil

Table 5 Summary of VES results along profile A in the study area for Field 3

VES point	Numbers of layers	Curve type	Resistivity of layers (**Ωm**)	Layer thickness (m)	Depth of layer (m)	Inferred lithology
B1	1	H	181.3	0.54	0.00	Topsoil
			40.63	2.74	0.54	
	2		1116	∞	3.29	Fresh basement
B2	1	H	63.69	1.59	0.00	Topsoil
			33.15	2.98	1.59	
	2		595.6	∞	4.57	Fresh basement
B3	1	A	79	1.8	0.00	Topsoil
			516	24.9	1.8	
	2		1696	∞	26.7	Fresh basement
B4	1	A	37.75	1.43	0.00	Topsoil
			466.9	6.81	1.43	
	2		1525	∞	8.23	Fresh basement
B5	1	A	71.43	1.30	0.00	Topsoil
			322.2	6.32	1.30	
	2		2696	∞	7.63	Fresh basement
B6	1	A	43.5	1.35	0.00	Topsoil
			237.3	5.83	1.35	
	2		2425	∞	7.18	Fresh basement

ascertained. To test the validity of this algorithm, two sites for VES are sited within the fracture region and the third one outside the fault zone to serve as a control.

Another factor considered in the choice of these methods is the rechargeability of the proposed boreholes; rechargeability has been linked to four traits which are falling runoff and rainfall amounts, rising atmospheric temperature, and population growth (Akurugu et al. 2020). This investigation has employed both magnetic and electrical resistivity methods in trying to resolve the identified problem. The use of integrated geophysical method for groundwater exploration in hard rock has yielded good results, (Bernard and Valla

Table 6 Summary of VES results along profile B in the study area for Field 3

VES point	Numbers of layers	Curve type	Resistivity of layers (**Ωm**)	Layer thickness (m)	Depth of layer (m)	Inferred lithology
B1	1	H	181.3	0.54	0.00	Topsoil
			40.63	2.74	0.54	
	2		1116	∞	3.29	Fresh basement
B2	1	H	63.69	1.59	0.00	Topsoil
			33.15	2.98	1.59	
	2		595.6	∞	4.57	Fresh basement
B3	1	A	79	1.8	0.00	Topsoil
			516	24.9	1.8	
	2		1696	∞	26.7	Fresh basement
B4	1	A	37.75	1.43	0.00	Topsoil
			466.9	6.81	1.43	
	2		1525	∞	8.23	Fresh basement
B5	1	A	71.43	1.30	0.00	Topsoil
			322.2	6.32	1.30	
	2		2696	∞	7.63	Fresh basement
B6	1	A	43.5	1.35	0.00	Topsoil
			237.3	5.83	1.35	
	2		2425	∞	7.18	Fresh basement

Table 7 Summary of resistance and depth across geologic sections for Field 1

VES profile	Minimum resistivity (Ωm)	Maximum resistivity (Ωm)	Thickness of overburden (m)	Remark
A	171	81	40.5	Viable
B	94.8	2001.4	30.0	Viable
C	10.00	645.20	26.0	Viable
D	230.1	5993.95	13.2	Not viable
E	157.6	32.2	20.0	Viable

1991; Ronning et al. 1995; Kaikkonen and Sharma 1997; Ramtek et al. 2001; Krishnamurthy et al. 2003; Sharma and Baranwal 2005; Porsani et al. 2005; Yadav and Shashi 2007).

Geology of the study area

The geology of the Bosso local government area (Figs. 2 and 3) is part of Sheet 164 of the Nigerian basement complex. This Cratonic Plate occupies more than 61% of Nigeria's land mass. The rock types found within Bosso local government consist of coarse-grained biotite granite and granodiorite, cross-bedded by Schists. The granite types and the granodiorite form part of the Nigerian older granite (Obaje 2009). These Precambrian rocks consisting of crystalline rock series were formed during the Pan-Africa Orogeny. The older granite consists of pegmatite, quartz veins, porphyritic granites, and gneisses are present. In this Basement region, groundwater can only be found in the cracks and fractures of the local rock. Groundwater yield depends on the size of fractures and their interconnectivity (Sharma and Baranwal 2005).

Table 8 Summary of resistance and depth across geologic sections for Field 2

VES profile	Minimum resistivity (Ωm)	Maximum resistivity (Ωm)	Thickness of overburden (m)	Remark
A	296.9	770.2	39.4	Viable
B	320.9	1120	50.4	Viable
C	116.5	489.6	25.1	Viable
D	31.3	778.8	40.5	Viable
E	458.9	1078.9	42.1	Viable
F	274.7	1046	24.3	Viable

Materials and method

Materials

The materials used are as follows: Aeromagnetic data, Terrameter (ABEM SAS 1000), Pegs, hammer, electrodes, tapes, clips, and data recording sheets.

Theory of method

Vertical derivative

A derivative that attenuates long wavelength enhanced shallow features and discontinuity in magnetic trends. This helps in mapping subsurface structures such as fault, fractures, contact, and intrusive bodies (Geosoft Inc 2015).

$$L(r) = r^n \tag{1}$$

n signifies the order of differentiation, while r measured in radians/ground_unit is the wavenumber, where $r = 2pk$, the k is cycles/meters for this survey.

Theory of electrical resistivity

The process of electrical resistivity investigation involves sending electrical current, I, via a current electrode, C1 and C2, and the returning electrical signal (voltage) is measured across the two ends of the potential electrodes P1 and P2 which turns out to be the potential difference, V. The most applicable arrangements include Wenner, Schlumberger, Pole-pole, and Dipole–dipole arrays. The basic relationship for the electrical resistivity method obtained from Ohm's law is (Grant and West 1965; Dobrin and Savit 1988; Nwankwo 2011) the following:

$$\rho = \frac{RA}{L} \tag{2}$$

Rho, ρ is the resistivity, R signifying the resistance, L for the length of a homogenous conducting cylinder of cross-sectional area A. Because the earth is anisotropic in nature, Eq. (2) can be further transformed as follows:

$$\rho_a = \frac{\Delta V}{I} 2\pi r \tag{3}$$

where $2\pi r$ represents the geometric factor, K (K is constant for every electrode configuration). Schlumberger array was employed in this research with a geometrical factor given as follows:

Table 9 Summary of resistance and depth across geologic sections for Field 3

VES profile	Minimum resistivity (Ωm)	Maximum resistivity (Ωm)	Overburden thickness (m)	Remark
A	358	1850	9.99	Not viable (shallow and high resistivity)
B	40.63	1696	26.16	Not viable (shallow and high resistivity)
C	190.5	3517	45.88	Not viable (high resistivity)
D	103.6	1173	8.09	Not viable (shallow and high resistivity)
E	150.3	1585	36.91	Not viable (shallow and high resistivity)
F	32.76	338.8	36.89	Not viable (shallow and high resistivity)

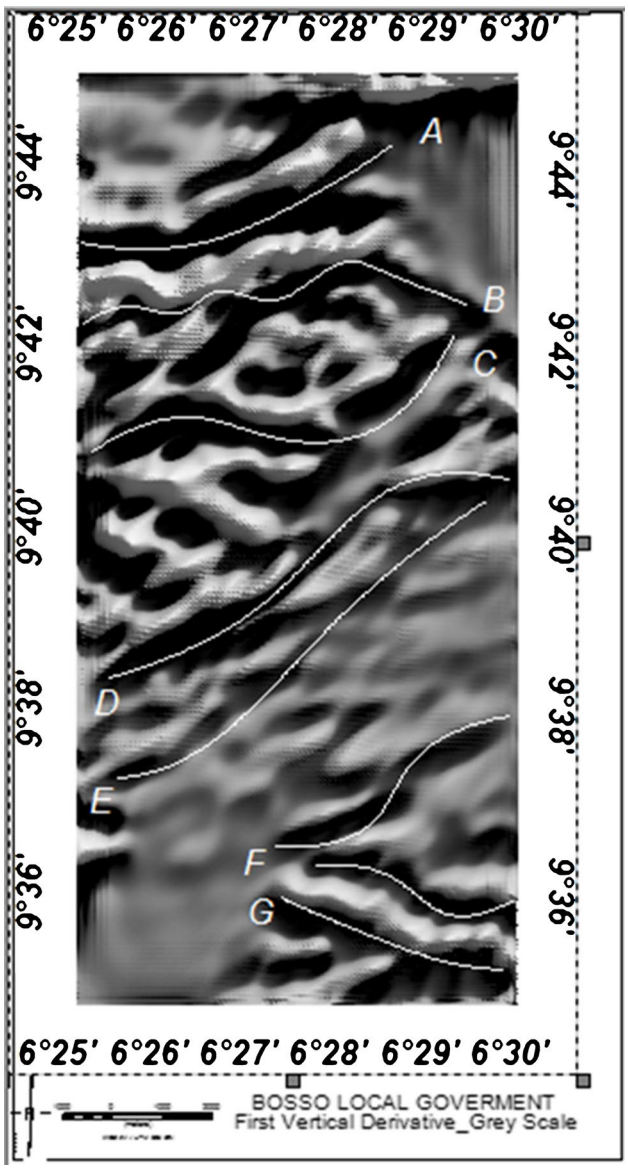

Fig. 4 First vertical derivative map of the study area showing delineated structure

$$\rho_a = \frac{\Delta V}{I} 2\pi r \tag{4}$$

The apparent resistivity, ρ_a is the bulk average of all rock and soil influence on the motion of the applied current (Telford et al. 1990; Ward 1990; Arsène et al. 2018).

The Vertical Electrical Sounding method using the Schlumberger array was chosen for this study area because it has proven to be an economic, quick, and effective means of solving most groundwater problems in different parts of the world (Breusse 1963; Zohdy and Jackson 1969; Frohlich 1974). Among the geoelectrical methods, Vertical Electrical Sounding techniques have been frequently used in hydrogeophysical studies for groundwater in both porous and fissured media (Onuoha and Mbazi 1988; Mbonu et al. 1991; Franjo et al. 2003). This method is based on the response of the earth to the flow of regulated input DC current source.

Procedure

The total magnetic data was processed for regional/residual separation and the residual field was reduced to the equator and fast Fourier transform (FFT). Then first vertical derivative algorithm is applied in the frequency domain to delineate and map the faults, fractures, and contacts.

Three sites were chosen where geoelectrical investigation for groundwater was carried out; sites A and B are within the fractured zones and site C is outside the fractured zone which serves as a control. Site A is at Day Secondary School, Kampala, 12 km from Maikunkele town, on latitudes 9° 40′ 37.11″ to 9° 41′ 37.1″ N and longitudes 6° 29′ 52.64″ to 6° 30′ 51.56″ E. Site B is 2 km from Maikunkele, close Day Secondary School.

Maikunkele, on latitudes 09° 40′ 37.17″ to 09° 41′ 37.15″ N and longitudes 06° 29′ 51.66″ to 06° 30′ 51.55″ E, and site C is roughly 1 km from the International Airport. Thirty-six (36) VES points were sampled on each of the three sites namely A (site 1), B (site 2), and C (site 3). This is achieved

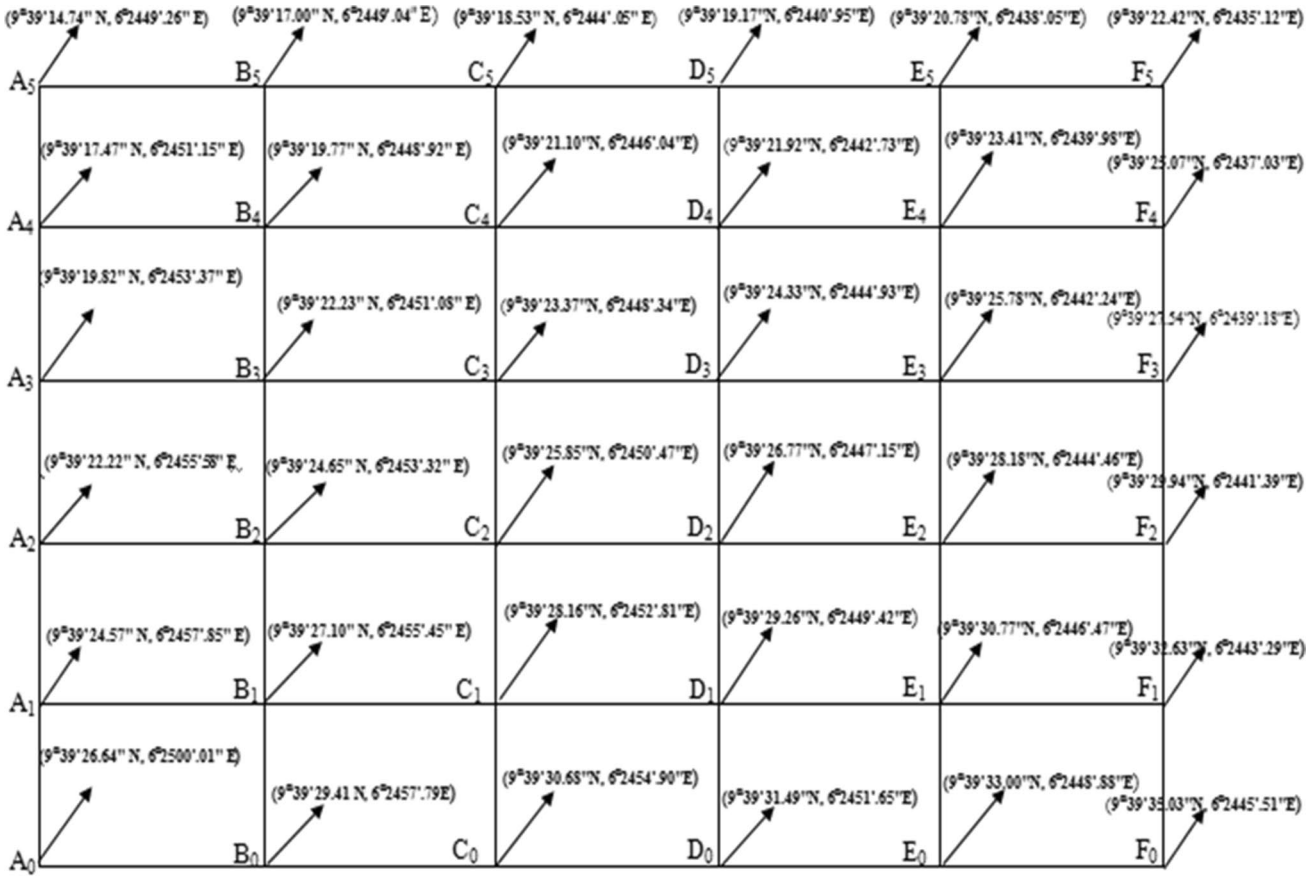

Fig. 5 Profile layout indicating coordinates for Vertical Electrical Sounding data collection

by dividing the 500 by 500 m plot into six profiles at an interval of 100 m and an inter-profile distance of 100 m. The appropriate coordinates of each VES point were established using the GPRS. Using the Schlumberger array and half current electrode (AB/2) of 1 to 100 m, values of current and the corresponding potential difference were collected on each VES point (Sharma and Baranwal 2005; Arsène et al. 2018). The log–log curve of the apparent resistivity versus AB/2 values was achieved using a computer program, called WinResist software, each of these curves gives the

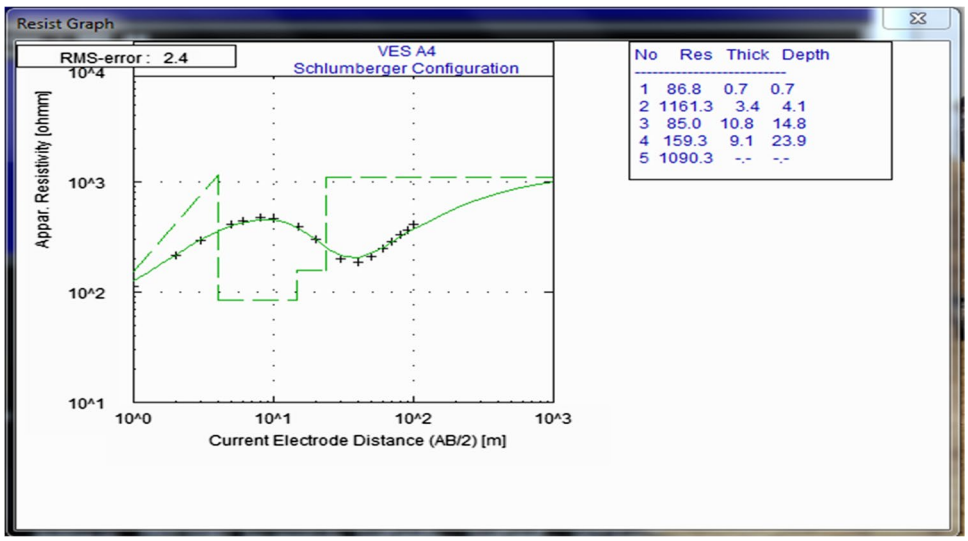

Fig. 6 A typical WinResist curve for VES for point A4 Field one or A

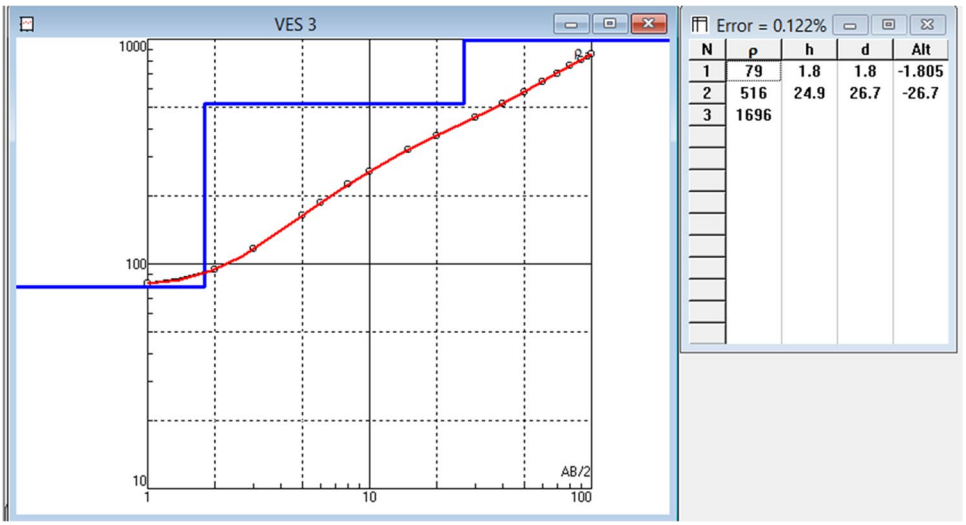

Fig. 7 Curve of VES point 3 on profile B Field 3 or (C)

equivalent *n*-layered model from the apparent resistivity and depth of each sounding point. Employing the result from the WinRest curve which provides the depth versus resistivity value, the observed geology on the field and table of rock resistivity, Tables 1, 2, 3, 4, 5, and 6, was generated that corresponds to VES on profiles A, B, and C for Field (1 or A), Field (2 or B), and Field (3 or C). Similar tables exist for the remaining profiles C, D, and E on each of the three fields.

From the various VES tables, a summary of the result of minimum and maximum depth across each profile was produced giving rise to Tables 7, 8, and 9, from which the viability of the VES point could be predicted. Equally from the tables, depth to basement rocks was estimated, and using Surfer 11 computer software, a contour map of depth to basement map was generated, for example, Fig. 4 is that for site 3 or C. This gives more information about the depth and location of both viable and non-viable VES points.

Analysis and results

The Total Magnetic Intensity data obtained from the Nigerian Geological Survey Agency (NGSA) had been corrected for magnetic compensation, noise removal, diurnal removal, micro levelling, and IGRF of 33,000 nT removed. The resultant data was subjected to regional residual separation by employing the polynomial fitting method, the residual field was reduced to the equator to attenuate the data's dependence on the angle of inclination, and finally, first vertical derivatives were applied to obtain and map major structures and lineament within the area.

The anomalous magnetic field map of the study area in Fig. 5 portrayed regions of positive and negative magnetic anomalies which characterized near-surface structure such as outcrops and thick sedimentation (Adetona and Mallam 2013). Susceptibility values range from – 164.316 nT to 222.725 nT. Major structures within sheet 164 trend in the NE-SW and N-W directions.

Regions that display weak magnetic susceptibilities qualify for a fitting environment for groundwater recharge, while formations with high apparent susceptibilities control groundwater flow from escaping the point of recharge (Rangganai and Ebinga 2008; Otlaadisa et al. 2022). The anomalous magnetic field data subjected to vertical derivative identifies a set of fault lines denoted as (A, B, C, D, E, F, and G) majorly trending in the Northeast–Southwest directions (Fig. 6). A is situated below latitude 9.45′ just after Maikunkele village; it demarcates the low susceptibility region at the upper part of the field from the lower region through Kangwo, Nini, Lawo, and other communities. B lies on latitude 9.43′ and terminates at about 2 km before Kuyi village. C lies on latitude 9.40′ below Maikunkele and goes down through Nanaum. D sat on latitude 9.38′ few kilometres from major settlements.

Interpretation of some geoelectric and geological section along profiles

Geologic section through profile A Field 1

The geologic and geoelectric section through profile A_F1, from Table 1. The geologic section has three lithological units. The first layer has thickness/depth ranges between 0.6 and 1.8 m, with resistivity ranging between 1.4 and 271 Ωm. The second section has depth variation between 20.2 and 38.5 m, and its resistivity varies between 132 and 1065 Ωm. The third layer has depth variation between 20.8 and 39.4 m, resistivity of this layer ranges from 5.6 to 2256 Ωm.

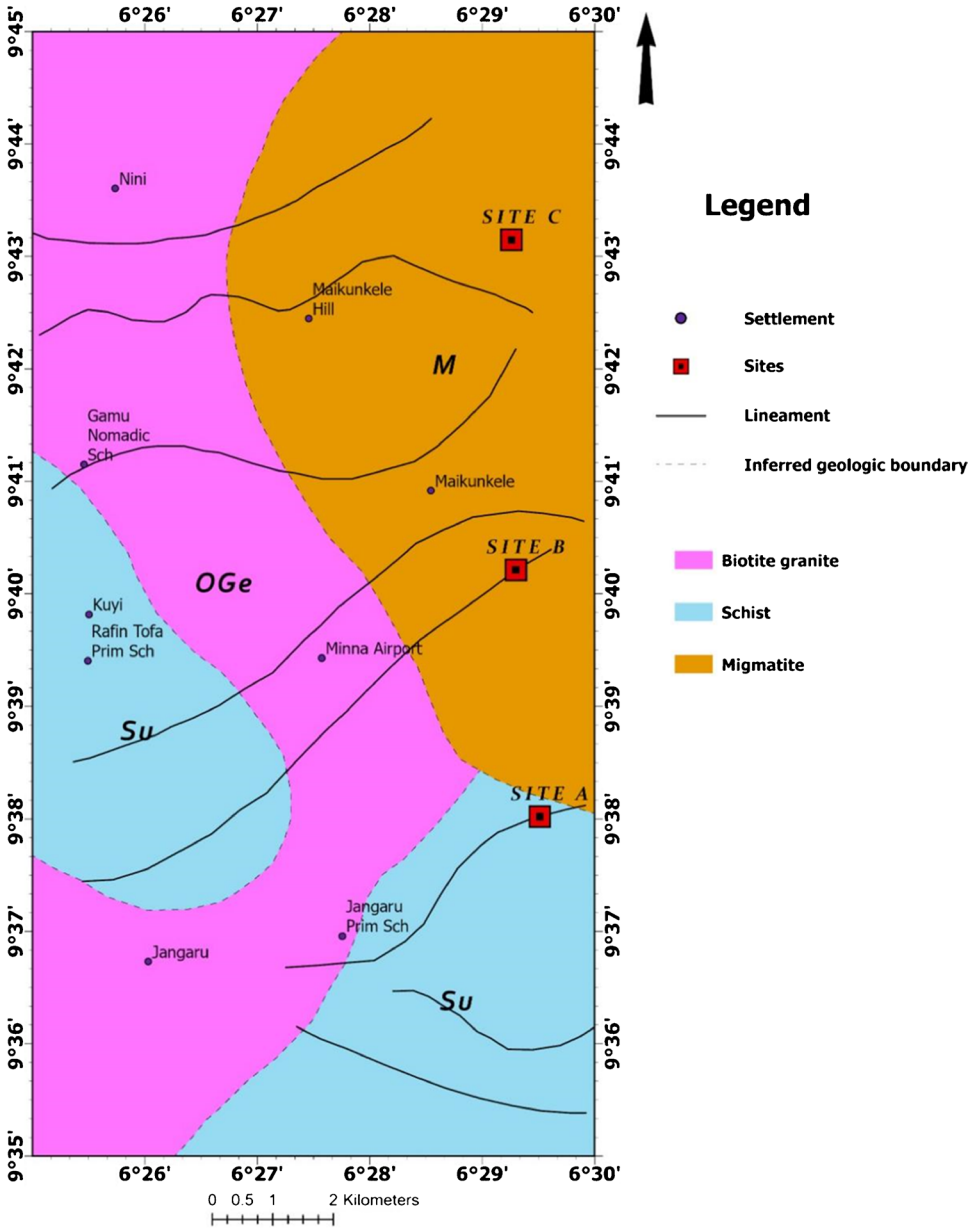

Fig. 8 Lineaments superimposed on geology map with survey sites

Geologic section through profile A Field 2

The geologic and geoelectric section through profile A_F2, from Table 3. The geologic section has three lithological units. The first layer has thickness/depth ranges between 0.6 and 1.8 m, with resistivity ranging between 13.4 and 410 Ωm. The second section has depth variation between 20.2 and 38.5 m, and its resistivity varies between 197.2 and 417 Ωm. The third layer has depth variation between 20.8 and 39.4 m, resistivity of this layer ranges from 266.4 to 4541 Ωm.

Geologic section through profile B Field 1

The geologic and geoelectric section through profile B_F1, from Table 2. The geologic section has three lithological units. The first layer has thickness/depth ranges between 0.6 and 8.7 m, with resistivity ranging between 45 and 281 Ωm. The second section has depth variation between 6.6 and 41.7 m, and its resistivity varies between 53 and 4105 Ωm. The third layer has depth variation between 7.2 and 50.4 m, resistivity of this layer ranges from 884 to 9949 Ωm.

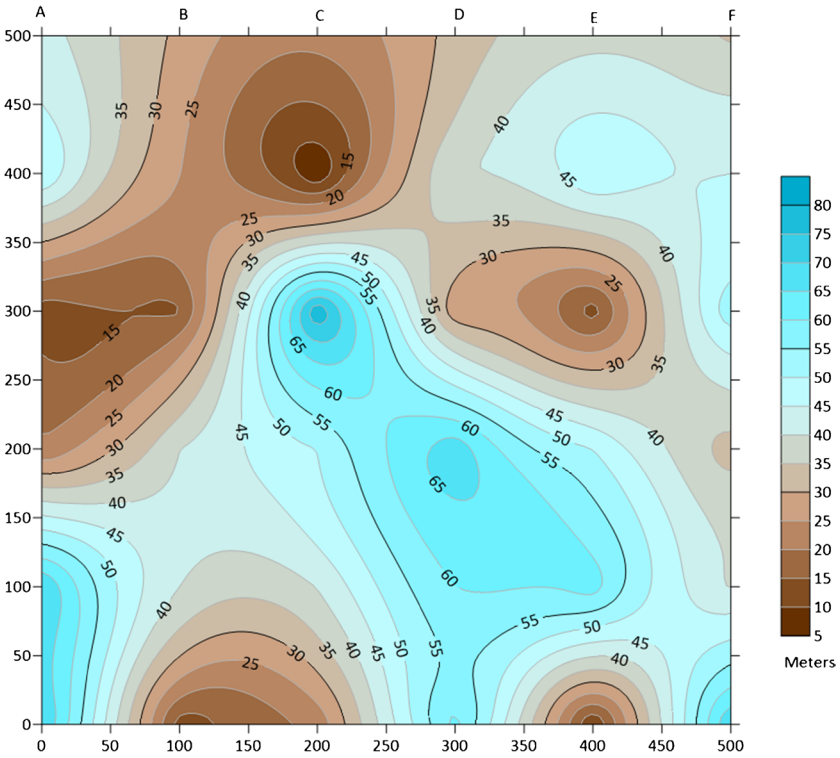

Fig. 9 Depth to fresh basement rocks for site A_Kampala Village

Geologic section through profile B Field 2

The geologic and geoelectric section through profile B_F2, from Table 4. The geologic section has three lithological units. The first layer has thickness/depth ranges between 0.6 and 8.7 m, with resistivity ranging between 40.2 and 372.5 Ωm. The second section has depth variation between 6.6 and 41.7 m, and its resistivity varies between 272.5 and 589 Ωm. The third layer has depth variation between 7.2 and 50.4 m, resistivity of this layer ranges from 171 to 3011.7 Ωm.

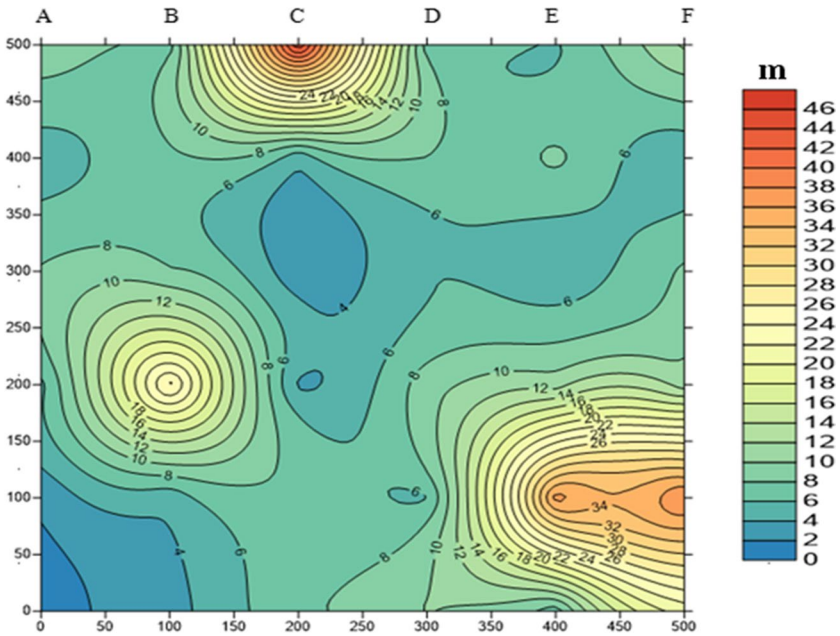

Fig. 10 Depth to fresh basement rocks for site B_Maikunkele Village

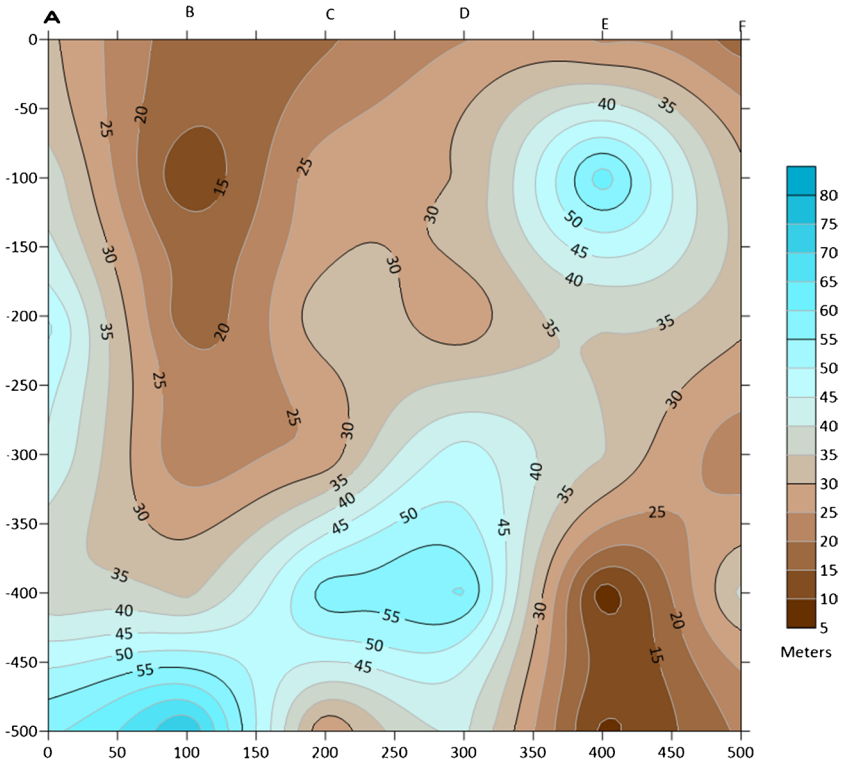

Fig. 11 Depth to fresh basement rocks for site C_control

Conclusion

The Anomalous Magnetic Field data was subjected to vertical derivative. This reveals a set of lineaments labelled (A, B, C, D, E, F, and G) which trend in the Northeast–Southwest directions (Fig. 7). A lies just below latitude 9.45′ just above Maikunkele village; it demarcates the low susceptibility region at the upper part of the field from the lower region through Kangwo, Nini, Lawo, and other communities. B lies on latitude 9.43′ and terminates at about 2 km before Kuyi village. C lies on latitude 9.40′ below Maikunkele and goes down through Nanaum. D sat on latitude 9.38′, interestingly no community within this region where the fault passes through.

The apparent resistivity values and the corresponding depth were used to build the geologic sections which revealed the existence of three subsurface layers. The layers comprise topsoil, intermediate clay formation, and weathered/fractured or fresh basement (Tables 1, 2, 3, 4, 5, and 6). The depth to basement map was also produced, (Figs. 8, 9 and 10); for Field (C or 3), the interpretation reveals a very shallow depth to basement rocks; only three VES points have depth in the range of 20 m; depth to basement within VES A2, B5, D2, and E1 on Field 1 or A are relatively higher; depth values range between 35 and 45 m while the shallow regions of the area have a depth range value between 15 and 20 m; similar results to that of site A was obtained on site B. Hence, VES A_2, A_5, B_4, B_5, C_2, C_4, D_4, D_5, E_1, E_3, and F_4 are marked as a conductive zone which are prolific for groundwater potential.

The depth range for aquifer potential zones is between 22.7 and 50.4 m. Result from site C (control) is quite different as two (2) layers were delineated in the VES points; depth to basement in roughly 90% of the VES points falls below 8 m; only three VES points that show appreciable depths are B3, C_6, and F_2 with depths ranging between 20 and 30 m, (Fig. 10); they are disregarded due to lack of connectivity which could hamper chargeability (Yadav and Shashi 2007; Rangganai and Ebinga 2008). Figure 11 shows the orientation of lineaments and positions of survey stations (A, B, and C) on the geology map.

Recommendations

This research work has demonstrated the efficacy of using integrated geophysical method in exploring for groundwater within the basement region in which the desired water can only be reached through faults and fractures. From the results, it is recommended that any boreholes sunk within site A (one) and B (two) (Fig. 8) are expected to give a good yield if the right coordinate is taken into consideration. There is the need to carry out Vertical Electrical Sounding within the fault line delineated as (A), above Maikunkele Hill, which is located at a higher altitude relative to the axis where the groundwater is required; having water here will solve the problem of pumping the water upward to where it is required.

Supplementary Information The online version contains supplementary material available at https://doi.org/10.1007/s12517-023-11784-5.

Acknowledgements Appreciation goes to the Nigerian Geological Survey Agency for the provision of magnetic data for this survey.

Declarations

Conflict of interest The authors declare no competing interests.

References

Adetona AA, Mallam Abu (2013) Estimating the thickness of sedimentation within lower benue basin and upper Anambra Basin, Nigeria, using both spectral depth determination and source parameter imaging Hindawi Publishing Corporation ISRN. Geophysics 2013(Article 124706):10. https://doi.org/10.1155/2013/124706

Akurugu BA, Chegbeleh LP, Yidana SM (2020) Characterisation of groundwater flow and recharge in crystalline basement rocks in the Talensi District, Northern Ghana. J Afr Earth Sc 161:103665. https://doi.org/10.1016/j.jafrearsci.2019.103665

Alile MO, Jegede SI, Ehigiator OM (2008) Underground water exploration using electrical resistivity method in Edo State. Nigeria Asian J Earth Sci 1:38–42

Anudu GK, Onuba LN, Ufondu LS (2011) Geoelectric sounding for groundwater exploration in the crystalline basement terrain around Onipe and adjoining areas, southwestern Nigeria. J Appl Technol Environ Sanitation 1(4):343–54

Ariyo SO, Adeyemi GO (2009) Role of electrical resistivity method for groundwater exploration in hard rock areas: a case study from Fidiwo/Ajebo areas of Southwestern Nigeria. Pac J Sci Technol 10(1):483–486

Arsène M, Wassouo Elvis BW, Daniel G, Théophile NM, Kelian K, Daniel NJ (2018) Hydrogeophysical investigation for groundwater resources from electrical resistivity tomography and self-potential data in the Méiganga Area, Adamawa, Cameroon. Int J Geophys 1:2018. https://doi.org/10.1155/2018/2697585

Bernard J, Valla PG (1991) Groundwater exploration in fissured media with electrical and VLF methods. Geoexploration 27:81–91

Breusse JJ (1963) Modern geophysical methods for subsurface water exploration. Geophysics 28(4):633–57

Dobrin MB, Savit CH (1988) Introduction to geophysical prospecting. McGrraw-Hill Companies

Franjo SU, van Kosta ID (2003) Hydrological mapping of moicene aquifer by 2-D electrical imaging. Rudavsko-Geolosko Naftm-Zbornik 15:19–29

Frohlich RK (1974) Combined geoelectrical and drill-hole investigations for detecting fresh-water aquifers in northwestern Missouri. Geophysics 39(3):340–352

Grant FS, West GE (1965) Interpretation theory in applied geophysics. McGraw-Hill, New York. https://doi.org/10.1017/S0016756800050627

Inc G (2015) Oasis Montaj MAGMAP how-to guide. Geosoft Incorporated, Toronto

Kaikkonen P, Sharma SP (1997) Delineation of near-surface structures using VLF and VLF-R data-an insight from the joint inversion result. Lead Edge 16(11):1683–1686

Krishnamurthy NS, Kumar D, Rao Anand V, Jain SC, Ahmed S (2003) Comparison of surface and sub-surface geophysical investigations in delineating fracture zones. Curr Sci 84(9):1242–1246

Lowrie W (1997) Fundamentals of geophysics. Cambridge Press, London

Mbonu PDC, Ebeniro JO, Ofoegbu CO, Ekine AS (1991) Geoelectric sounding for the determination of aquifer characteristics in parts of the Umuahia area of Nigeria. Geophysics 56(2):284–291

Nwankwo LI (2011) 2D resistivity survey for groundwater exploration in a hard rock terrain: A case study of MAGDAS observatory, UNILORIN, Nigeria. Asian Journal of Earth Sciences 4(1):46

Nwankwo LI, Olasehinde PI, Babatunde EB (2004) The use of electrical resistivity pseudo-section in elucidating the geology of an east-west profile in the basement complex terrain of Ilorin, West-Central Nigeria. Nig J Pure Appl Sci 19:1672–1682

Obaje NG (2009) Geology and mineral resources of Nigeria. Springer, Dordrecht Heidelberg London New York, p 221

Olasehinde PI (1999) An integrated geological and geophysical exploration techniques for groundwater in the basement complex of west central part of Nigeria. J Natl Assoc Hydrogeologist (water Resources) 10(1):46–49

Onuoha KM, Mbazi FC (1988) Aquifer transmissivity from electrical sounding data: the case of Ajali Sandstone aquifers southwest of Enugu, Nigeria. Groundwater and mineral resources of Nigeria. Vieweg, Braunschweig, Germany 17–29

Otlaadisa T, Ranganai RT, Ditiro BM, Kealeboga KM, Joyce GM (2022) Investigating groundwater recharge potential of Notwane catchment in Botswana using geophysical and geospatial tools. J Hydrol: Regional Studies 40:101011. https://doi.org/10.1016/j.ejrh.2022.101011

Oyedele KF, Ogagarue DO, Esse O (2011) Groundwater potential evaluation using surface geophysics at Oru-Imope, South-Western Nigeria. Eur J Sci Res 63(4):515–522

Plummer CC, Mc Geory D, Carlson DH (1999) Physical geology, 8th edn. McGraw Hill Co., Inc., New York, pp 48–56

Porsani JL, Vagner RELF, Yukio H (2005) Geophysical investigations for the characterization of fractured rock aquifers in Itu, SE Brazil. J Appl Geophysics 57(2 2005):119–128

Ramtek RS, Venugopal K, Ghish N, Krishnaiah C, Panvaikar GA, Vaidya SD (2001) Remote sensing and surface geophysical techniques in the exploration of groundwater at UshaIspat Ltd., Sindhurg Dist., Maharastra India. J IGU 5(1):41–49

Rangganai RT, Ebinga CJ (2008) Aeromagnetic and Landsat TM structural interpretation for identifying regional groundwater exploration targets, south-central Zimbabwe Craton. J Appl Geophysics 65:73–83. https://doi.org/10.1016/j.jappgeo.2008.05.009

Ronning JS, Lauritsen T, Mauring E (1995) Locating bedrock fractures beneath alluvium using various geophysical methods. J Appl Geophy 34(137):167

Sharma SP, Baranwal VC (2005) Delineation of groundwater-bearing fracture zones in a hard rock area integrating very low frequency electromagnetic and resistivity data. J Appl Geophys 57(2):155–166. https://doi.org/10.1016/j.jappgeo.2004.10.003

Singh KKK, Singh AKS, Singh KB, Sinha A (2006) 2D resistivity imaging survey for siting water-supply tube well in metamorphic terrains: a case study of CMRI campus, Dhanbad, India. Lead Edge 25:1458–1460

Telford WN, Geldart LP, Sheriff RE (1990) Applied geophysics (2nd Ed) Cambridge. Appl Sci (ZJPAS) 7(1):52–58

Ward SH (1990) Resistivity and induced polarization methods in geotechnical and environmental geophysics. Society of Exploration Geophysicists, Tulsa, pp 147–189

Water for Africa, 2010. http://www.waterforafrica.org.uk/

Yadav GS, Shashi KS (2007) Integrated resistivity surveys for delineation of fractures for ground water exploration in hard rock areas. J Hydrol: Regional Studies. https://doi.org/10.1016/j.jappgeo.2007.01.003

Zohdy AA, Jackson DB (1969) Application of deep electrical soundings for groundwater exploration in Hawaii. Geophysics 34(4):584–600